Minerals Engineering 137 (2019) 68–77

Contents lists available at ScienceDirect

Minerals Engineering

journal homepage: www.elsevier.com/locate/mineng

Studying the integration of solar energy into the operation of a semi-autogenous grinding mill. Part I: Framework, model development and effect of solar irradiance forecasting

G. Pamparana[a,b], W. Kracht[a,b,*], J. Haas[c], J.M. Ortiz[d], W. Nowak[c], R. Palma-Behnke[e]

[a] Department of Mining Engineering, Universidad de Chile, Chile
[b] Advanced Mining Technology Center, AMTC, Universidad de Chile, Chile
[c] Department of Stochastic Simulation and Safety Research for Hydrosystems (IWS/SC SimTech), University of Stuttgart, Germany
[d] The Robert M. Buchan Department of Mining, Queen's University, Canada
[e] Energy Center, Department of Electrical Engineering, Universidad de Chile, Chile

ARTICLE INFO

Keywords:
Sustainable mining
Solar energy
Battery energy storage system
Semi-autogenous grinding mill

ABSTRACT

Grinding is one of the most energy-demanding processes of copper mines. Declining ore grades and harder rocks will further intensify this demand. Periods of stressed copper prices, high energy costs and climate change mitigation targets additionally motivate the search for alternative energy sources in mining. In Chile, many copper operations are located in the Atacama Desert, hence solar energy systems are an attractive solution. However, the mineral hardness is variable and uncertain in time and space, which adds challenges to planning energy systems with high solar shares. More specifically, here a stochastic optimization model is developed. It sizes the solar photovoltaic (PV), battery energy storage system (BESS) and the contracted power, based on the solar radiation, mineral hardness, and costs. Using Markov Chains, different years of solar radiation are generated from historical records. These solar scenarios are used to test the impact of individual years with long periods of cloudy/rainy days on the sizing of the system, in contrast to planning with an average year or planning with many-year time horizons in a stochastic approach. The novelties lie in the developed model, and in understanding the impact of the uncertainty and variability of rock hardness and solar irradiation on the optimal sizing of the PV-BESS system and the power capacity contract. Furthermore, the impact of a larger variability of ore hardness is evaluated in one scenario. PV-BESS can cost-effectively provide energy to the grinding mill. Different planning approaches lead to significant differences in the recommended power supply. In contrast to planning with the average solar year, using a conservative solar year (many cloudy days) yields significantly smaller sizes of PV and BESS (20% and 55%) and a higher reliance on the grid (larger contracts and imports); and the stochastic approach follows a similar line (10% and 25% smaller). Despite its increased grid dependency, the one-year stochastic approach provides more robust solutions regarding costs and sizes (avoiding penalties). The variability of the rock hardness also impacts the size of all components of the PV-BESS system, especially the battery energy capacity. Its relevance for battery sizing motivates to perform further studies with a focus on the uncertainty and variability of the ore.

1. Introduction

The progressive decline of mineral grade in many countries such as Chile has had several effects. For example, the costs to produce a metal unit have been rising in a progressive and significant way, and this affects the costs of mineral comminution (COCHILCO, 2013; Harmsen et al., 2013). Deeper mines have harder minerals, increasing the amount of energy required to grind them and to obtain the necessary mineral liberation (Topp, 2008; Norgate and Jahanshahi, 2010; Carrasco et al., 2016). Worldwide, the grinding process is one of the most energy-intensive processes (Wei and Craig, 2009). In Chile it corresponds, on average, to almost 50% of the electrical consumption of the copper process, from which the semi-autogenous grinding mill (SAG mill) is a significant component (COCHILCO, 2013). Several tests have been developed to predict their energy consumption from geometallurgical data such as the SAG Power Index (SPI) Test (Starkey and

* Corresponding author at: Department of Mining Engineering, Universidad de Chile, Chile.
E-mail address: wkracht@uchile.cl (W. Kracht).

https://doi.org/10.1016/j.mineng.2019.03.017
Received 10 October 2018; Received in revised form 24 January 2019; Accepted 18 March 2019
Available online 27 March 2019
0892-6875/ © 2019 Elsevier Ltd. All rights reserved.

Dobby, 1996; Jahani et al., 2012). These tests have been applied to diverse mines through the world for design and mine planning (Keeney et al., 2011; Burger et al., 2006; Wirfiyata and McCaffery, 2011; Amelunxen et al., 2012; Suazo et al., 2010; Alruiz et al., 2009; Bergholz and Schreder, 2003; Flores, 2005). Furthermore, mineral deposits are inherently variable regarding their geometallurgical characteristics, including their mineral hardness (Kojovic et al., 2010). Different deposit characteristics require different perspectives and design criteria, which include energy consumption (Starkey and Scinto, 2010; Kittler et al., 2011; Bueno et al., 2015). Due to this, and to the increasing relevance of CO_2 emissions (McLellan et al., 2012; Norgate and Haque, 2010), other sources of energy must be considered. Renewable energy technologies are widely accepted as a structural solution for reaching an economic, accessible and environmental-friendly power supply. But to also meet reliability criteria, such renewable systems need to increase their flexibility (Kondziella and Bruckner, 2016). This flexibility can be achieved on the generation-side with flexible technologies (conventional technology such as hydropower (Haas et al., 2015) or smart wind or photovoltaic systems (Rahmann et al., 2016)) and on the demand-side by scheduling load when energy is abundant (Pamparana et al., 2017). Other alternatives are expanding the transmission (Steinke et al., 2013) and energy storage infrastructure (Haas et al., 2017).

During the last years, solar photovoltaic systems have proliferated very quickly. From little under 50 GW of installed capacity worldwide in 2015 to over 400 GW by the end of 2017 (Ren21 et al., 2018), and over 500 GW were expected by 2018. As solar shares grow, so do storage technologies. The U.S Department of Energy, in its "global energy storage database", reports over 250 Li-ion projects over 1 MW (as of February 2018) (US Department of Energy, 2018). These include, to name a few recent examples, projects for grid support (100 MW by Tesla in South Australia), renewables capacity firming (40 MW Minami-Soma by Toshiba/Tohoku), ramping (32 MW Laurel Mountain by AES in West Virginia), distribution grid upgrade (30 MW Golden Hills by NextEra in California), voltage support and transmission congestion management (28 MW West-Ansung by Kepco/Kokam/LG in South Korea), and electric energy time shift (30 MW Escondido by SDG&E in California) (US Department of Energy, 2018).

Storage technologies have also been included in multiple expansion planning exercises, where investments into upgrades of power systems are being optimized. In fact, the reviews of references (Cebulla et al., 2018; Haas et al., 2017) looked at over 100 studies (and 400 scenarios) related to the design of future power systems with storage devices. Many of them include batteries (Viveka et al., 2015; Han et al., 2015). Other recent reviews (Zerrahn and Schill, 2017; Schill and Zerrahn, 2018) and studies also provide evidence for the cost-effectiveness of highly renewable systems with storage backup (Gulagi et al., 2017; Koskinen and Breyer, 2016).

In the copper mining sector, in particular, the literature is more scarce on designs of highly renewable systems. Nevertheless, there are some recent conference publications. For example, the development of converters for directly using the solar photovoltaic electricity in copper electrorefining (thus, avoiding the inverter) (Castillo et al., 2015); or estimating the potential of solar central towers for producing pyrometallurgical copper (Cruz-Robles et al., 2018). However, a holistic design of energy supplies is absent.

As it can be seen in the reviewed body of literature above, many studies are concerned with sizing PV-BESS systems. Many of them are for large-scale power systems, in which the demand is well studied, given the many decades of experience from power system operators worldwide. What is not fully understood yet, is how to optimally design a solar system for individual large energy consumers, where the demand is not as studied. Copper mining companies are one example here. Furthermore, as the solar share grows, the energy supply becomes more independent from the power backup provided by the large-scale power grid. This means that the reliability against the solar variability is of increasing relevance.

For these reasons, a framework is presented for optimal system planning, that combines a model for the energy demand of mines, a model for solar profiles, and a model for optimal sizing. The present study focuses on (i) describing the framework, (ii) understanding how the solar variability impacts the investment decisions, and on (iii) a preliminary exploration of how mineral variability impacts the sizing. A comprehensive description of the energy demand model for the mines, including a systematic assessment of mine scheduling, is out of the scope but can be found in Pamparana et al. (2019).

This work aims to link the inherent mineral variability with the required flexibility of the energy supply. In specific, the required sizing of the PV power plant in combination with BESS for energy storage (buffering fluctuations in demand and power production) and conventional power contract (as backup if storage is insufficient) for providing that flexibility, is investigated. Here, the PV-BESS system is sized to achieve cost reductions by reducing the need for buying peak power from the external large-scale power grid. The proposed framework is shown and the model is described in the methods section. Also, the solar model for the solar photovoltaic generation data is shown here. The next section shows the results and discussions of the model testing and presents a case study to account for the solar resource variability with a sample mineral feed. A modification of the mineral feed is applied to change its variance and study its effects is also presented in this section. Finally, the conclusions and outlook are presented.

2. Methods

A framework for operating a system composed of a SAG mill, PV and BESS (SAG-PV-BESS) is proposed to model the system. The modeling is done by using a linear stochastic optimization of investment and operation decisions. This minimizes the operational and investment costs (as annuities representing the yearly payments of the investment taken to present value) using one year of mineral feed and PV energy generation data. The costs are associated with the operation of the SAG-PV-BESS system including the contracted power and use of the external grid in peak hours.

A methodology is introduced to study the effects of the solar and mineral hardness variability over the sizing and operation of the SAG-PV-BESS system. Synthetic data is generated to test the model. On the one side, a solar model is proposed to create synthetic solar power generation years, using Markov Chains constructed from actual data. On the other hand, data is generated from a geometallurgical model, where several realizations built with geostatistical simulation are obtained to reproduce the SAG mill ore feed. In this work one set of feed realizations (considered to be representative) in conjunction with several solar years are used to, first, check the behavior and consistency of the model, and second, to analyze the impact of the solar resource on the plant sizing. Also, an inspection on how the mineral variability itself affects the sizing of the system is studied.

The whole framework scheme is summarized in Fig. 1. The solar model is explained in Section 2.1, while the optimal sizing model and its inputs are explained in Section 2.2. The Mining Model corresponds to the modeling of the mineral extraction using geostatistical simulations, and the further SAG mill feed management to achieve the demand-side management (DSM). This way, the energy consumption of the mill can be controlled as a way to look if a deeper integration of the solar energy can be achieved. The mining model is explained in the second part of this work (Pamparana et al., 2019).

2.1. Solar model

Solar irradiance data is obtained from the *Explorador Solar* developed by the Geophysics Department from the University of Chile in conjunction with the Energy Ministry of the Chilean Government (Ministerio de Energía de Chile, 2017). The same source incorporates a model for PV power plants, where a PV installation with single axis

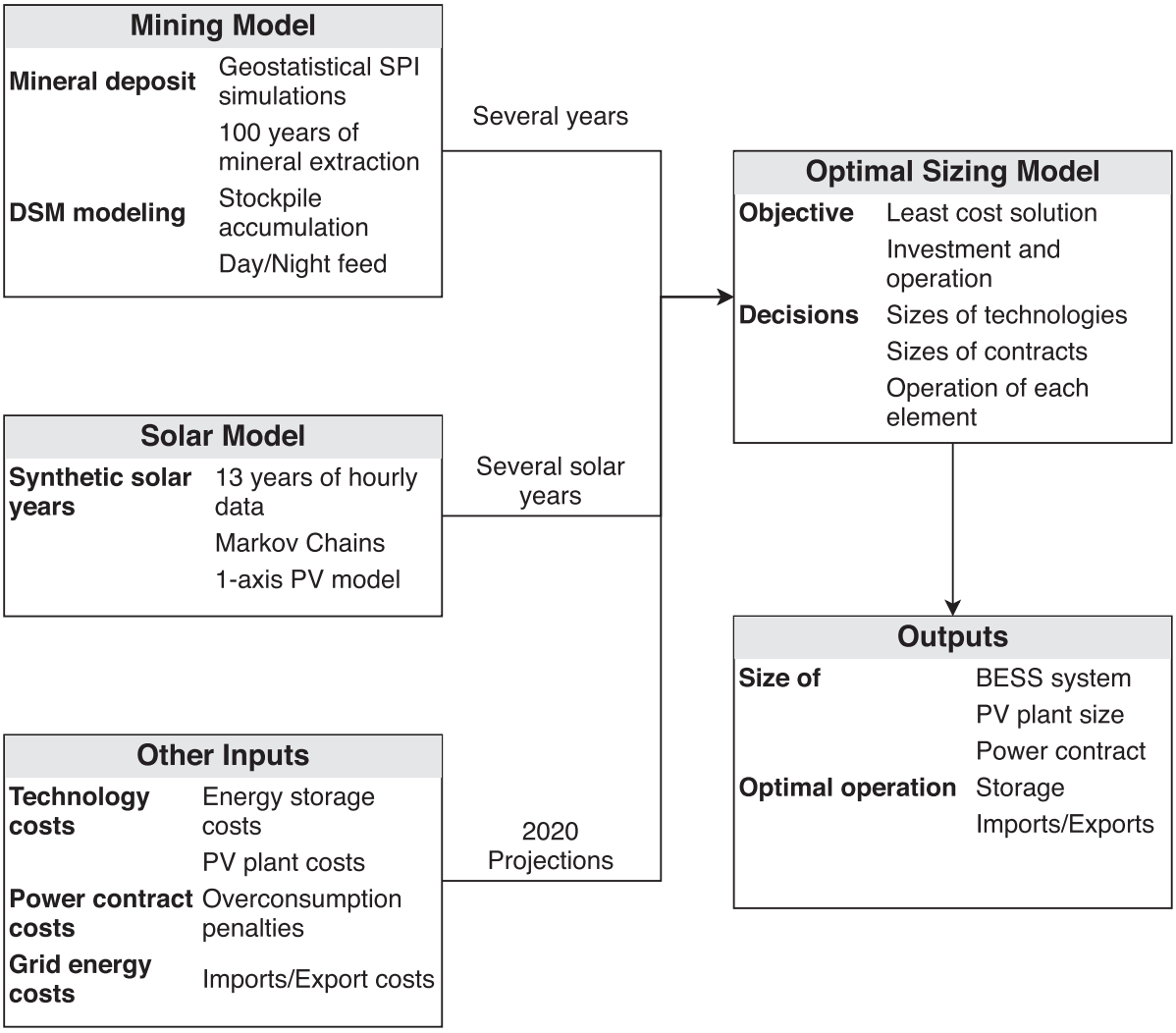

Fig. 1. Framework for sizing the PV system, BESS, and power contract: mining model, solar model.

tracking (E-W) is chosen (Molina et al., 2017). An inverter efficiency of 98%, plant energy losses of 10% (soiling and power transformation and transmission) and a temperature-coefficient of −0.5%/°C are considered. This generates annual power time series with an hourly resolution list for a specific location. This data is interpolated from installed climate measuring stations where data is available. In this way, 13 years of records are obtained for the location in the Chilean Atacama Desert with the coordinates LAT/LONG (−26.9808, −70.0214). From this data, the average and cloudy years are identified.

For the stochastic modeling, further synthetic years are generated by reshuffling historic days using Markov Chains. For this, four sunshine-classes are arbitrarily defined by using ratios (see Fig. 2) between the daily irradiation and the maximum possible sunshine of that day. The transition probabilities between the (daily) sunshine-classes are computed per month to capture seasonality. The classification is made in four categories called *Excellent*, *Good*, *Moderate*, and *Bad* depending on the obtained ratio and classified by the ranges shown in the table in Fig. 2. Following a Markov process, first, a sequence of 365 sunshine-classes is generated. Then, for each sunshine-class, a similar day is drawn from the historic data of that month. The following algorithm is used:

1. Daily irradiance records corresponding to each month are sorted to identify the highest irradiance value in the month. For example, for January, 31 records for each one of the 13 years is available, thus the maximum value out of the 403 records is found.
2. Daily irradiance records are classified according to four classes shown in the table in Fig. 2, where the range is computed relative to the highest irradiance day for the corresponding month computed in 1.
3. A transition probability matrix is calculated between four classes within each month. Table 1 shows the result for January.
4. For the Markov Chain simulation, a random day is used to initialize the algorithm in January. Transition probabilities within the corresponding month are used to simulate the forthcoming days, maintaining the expected transitions from the historic data, until a full year has been simulated.
5. To simulate the hourly irradiance variability, the hourly records of a day belonging to the same class and for the same month are drawn at random for each one of the 365 days simulated with the Markov Chain algorithm.
6. This process is repeated for the number of years needed.

The synthetic solar energy generation time series were validated by comparing them against the historic data regarding yearly solar irradiation, the variance between the different years and monthly change, and number and length of cloudy-days sequences. Details of these validations are not shown here due to space constraints. These data are used to generate a large database which is the input for the stochastic model. This way, several solar years are used to test the model in

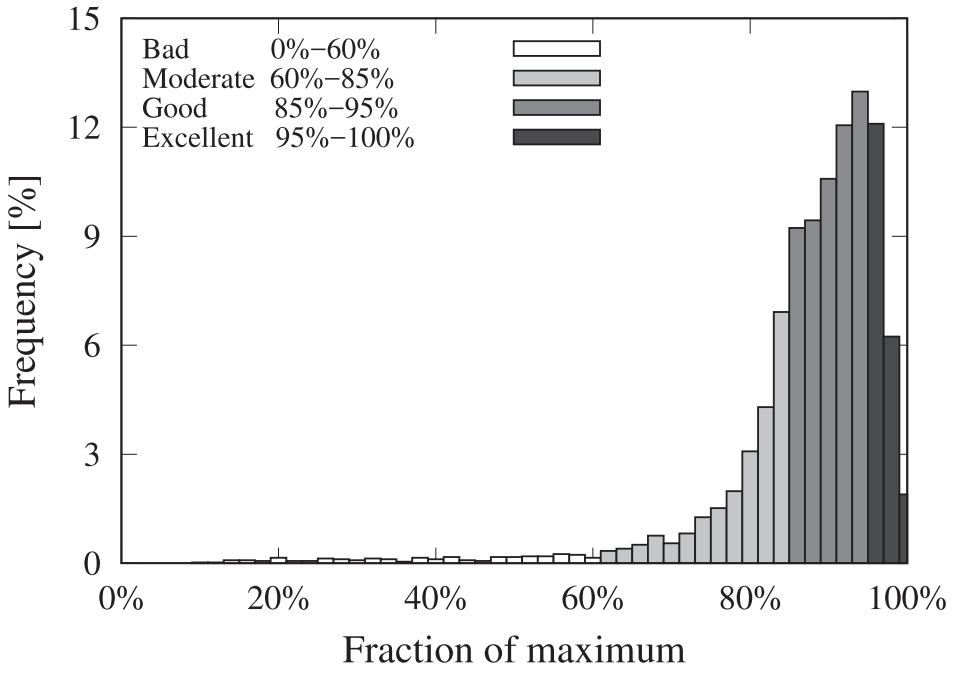

Fig. 2. Frequency histogram for the maximum daily irradiation fraction including classification.

Table 1
Resulting classification and transition matrix for the Markov Chains. January is shown as example.

From\To	Excellent	Good	Moderate	Bad
Excellent	12	12	2	0
Good	10	175	66	4
Moderate	3	65	49	0
Bad	1	2	1	0
From\To	Excellent	Good	Moderate	Bad
Excellent	46%	46%	8%	0%
Good	4%	69%	26%	2%
Moderate	3%	55%	42%	0%
Bad	25%	50%	25%	0%

different scenarios, either separately or at the same time.

2.2. Optimal sizing model

The optimal sizing model (details will follow in the subsequent sections) considers a system where a SAG mill operation is powered by the energy grid, a solar PV and BESS system. Energy imports and exports are permitted from the grid. The stochastic optimization problem minimizes the investment and operation costs. It considers 20 years of mining and solar data resulting from the solar and mining models, used as simultaneous inputs to the problem. The model takes into account the different technology costs (BESS and PV, using year 2020 cost projections), the power contract costs, including possible penalties for over-consumption, and energy coming from imports (buying costs) and exports (selling income) from the energy grid.

A diagram of the system can be seen in Fig. 3, which summarizes the energy balance of the process. Here, the SAG mill can be powered either by the power bought from the grid (imported), the power discharged by the BESS or the power generated by the PV plant. The BESS can be charged by either the power bought from the grid or the power generated by the PV plant. Finally, the excess energy in the system that is not stored or consumed by the SAG mill is sold to the grid (exported).

The results of the optimization model are the sizes of the PV and BESS system and the needed contracted power for the operation mentioned above, which are decision variables of the problem. Also, the optimal operation of the storage and the imports and exports from the grid are obtained.

The implementation was made using the GAMS® software platform and language, and using the CPLEX® solver link for the optimization.

2.2.1. Nomenclature

The nomenclature used is shown in Tables 2 and 3 for the decision variables and parameters, respectively. The convention used to describe them is to use upper case for parameters and lower case for variables.

2.2.2. Objective function

The objective function (to be minimized) are the total costs for one year (Eq. (1)). It considers the investment cost C^{inv}, the contracted power cost C^{con} and the expected value of the operational costs for several operational scenarios. As every considered year scenario has the same occurrence probability, the expected value is obtained by dividing the sum of yearly operational cost C_y^{op} by the number of considered years Y as seen in Eq. (2). In this model, it is sufficient and acceptable to fulfill in average the constraints using the expected value (Toscano, 2013).

$$minf = C^{inv} + C^{con} \cdot p^{con} + E(C_y^{op}) \tag{1}$$

$$E(C_y^{op}) = \frac{\sum_y C_y^{op}}{Y} \tag{2}$$

2.2.3. Investment costs

The investment costs shown in Eq. (3) are the generation costs $C^{inv,g}$ (Eq. (4)) and the storage costs $C^{inv,s}$ (Eq. (5)). These are the solar PV plant and the BESS investment costs (which include operation and maintenance costs) respectively for this work. They are transformed to annual costs by the annuity factor A. The variables for determining the costs are the size of the PV plant (power) p_{max}^g and the BESS energy capacity e_{max}^s.

$$C^{inv} = C^{inv,g} + C^{inv,s} \tag{3}$$

$$C^{inv,g} = Inv^g \cdot p_{max}^g \cdot A \tag{4}$$

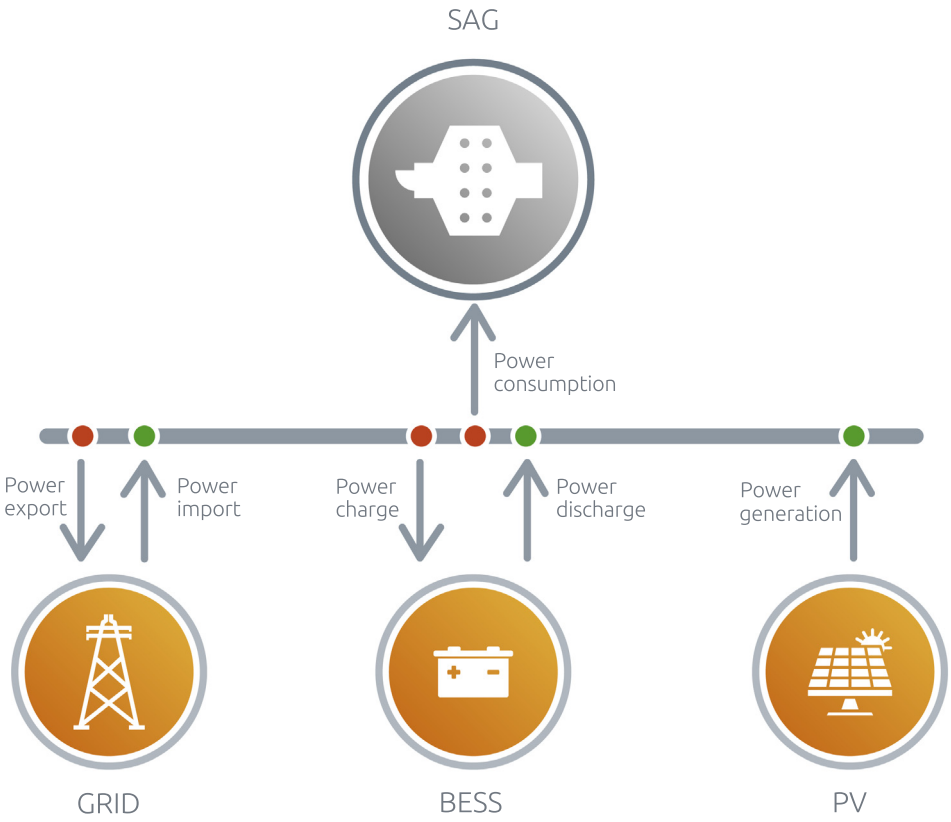

Fig. 3. Energy balance of the considered SAG-PV-BESS system.

Table 2
Decision variables nomenclature.

Variable	Description	Units
p^{con}	Contracted power capacity	MW
p^{g}_{max}	Maximum solar PV power	MW
e^{s}_{max}	BESS maximum energy capacity	MWh
e^{s}_{min}	BESS minimum energy capacity	MWh
p^{s}_{max}	BESS power capacity	MW
$p^{g}_{t,y}$	Power generated by PV system at time t of year y	MW
$p^{sch}_{t,y}$	Power charged to the batteries at time t of year y	MW
$p^{sdis}_{t,y}$	Power discharged from the batteries at time t of year y	MW
$p^{imp}_{t,y}$	Power imported from the grid at time t of year y	MW
$p^{exp}_{t,y}$	Power exported from the grid at time t of year y	MW
$p^{max,imp}_{y}$	Maximum power bought from the grid of year y	MW
$e^{s}_{t,y}$	Stored energy in BESS at time t of year y	MWh
$e^{sloss}_{t,y}$	BESS energy losses due to discharge amount and state of charge at time t of year y	MWh

$$C^{inv,s} = Inv^{s} \cdot e^{s}_{max} \cdot A \tag{5}$$

2.2.4. Operational costs

The operational costs C^{op}_{y} for each year scenario y subdivide into four costs as shown in Eq. (6). In order of appearance, they represent the generator, storage, grid, and penalties operational costs. Each of them depends on each data year considered in the study.

$$C^{op}_{y} = C^{g}_{y} + C^{s}_{y} + C^{grid}_{y} + C^{pen}_{y} \tag{6}$$

Eq. (7) shows the solar generation operation cost, which correspond to the maintenance solar PV plant.

Table 3
Parameters nomenclature.

Parameter	Description	Units
$P^{SAG}_{t,y}$	SAG mill power consumption at time t of year y	MW
Y	Number of years for stochastic simulation	–
A	Annuity factor	–
C^{con}	Yearly contracted power capacity cost	US$/MW
Inv^{g}	Solar PV plant investment cost	kUS$
Inv^{s}	BESS investment cost	kUS$
$C^{op,g}$	Solar PV plant operational costs	US$/MWh
$C^{rep,s}$	BESS replacement cost	US$/MW
N^{cycles}_{max}	BESS lifetime measured in cycles	–
Soc_{min}	BESS minimum state of charge	–
C^{imp}	Purchase price of energy	US$/MWh
C^{exp}	Selling price of energy	US$/MWh
$C^{penalty}$	Penalty for power over consumption	US$/MW/year
$P^{g,profile}_{t,y}$	PV power generation profile at time t of year y	MW
PE_{ratio}	BESS power/energy ratio	–
η^{sch}	Charging efficiency of BESS	–
η^{sdis}	Discharging efficiency of BESS	–

$$C^{g}_{y} = \sum_{t} \left(C^{op,g} \cdot p^{g}_{t,y} \cdot dt \right) \tag{7}$$

Eq. (8) shows the storage operational costs, which correspond to the BESS costs. It considers the battery replacement costs per MW of BESS, $C^{rep,s}$. This is established as the BESS' cycling based on a maximum number of cycles permitted and the depth of discharge. The cycles are defined by the used energy (either charge or discharge) divided by the BESS power capacity.

$$C_y^s = \sum_t \frac{\left(p_{t,y}^{sch} + p_{t,y}^{sdis}\right)\cdot C^{rep,s}\cdot p_{max}^s \cdot dt}{2\cdot N_{max}^{cycles}\cdot p_{max}^s\cdot(1 - Soc_{min})} \quad (8)$$

Eq. (9) shows the electrical grid operational costs which correspond to the imported and exported energy ($p_{t,y}^{imp}$ and $p_{t,y}^{exp}$, respectively) from it.

$$C_y^{grid} = \sum_t \left(p_{t,y}^{imp}\cdot C^{imp} - p_{t,y}^{exp}\cdot C^{exp}\right)\cdot dt \quad (9)$$

Eq. (10) shows the penalties costs associated with the energy over-consumption from the electrical grid. The mining companies have contracted power as upper limits in which they maintain the cost of energy. Electrical companies charge a high-cost penalty for over-consumption. For this reason, mining companies are drawn to contract higher power although they do not need that quantity. Here, the penalty is applied as a yearly cost calculated with the highest over-consumption incurred over the year.

$$C_y^{pen} = \left(p_y^{max,imp} - p^{con}\right)\cdot C^{penalty} \quad (10)$$

2.2.5. PV plant constraints

Eq. (11) calculates the PV power generation profile $p_{t,y}^g$ used in the simulations that corresponds to an amplification of a 1 MWp (Mega Watt peak, which is the maximum output of the PV plant) base profile $P_{t,y}^{g,profile}$ (that is generated using the solar model). This base profile is amplified by the PV plant size p_{max}^g (that is calculated within the optimization). This value is used to amplify every base profile scenario considered. The generated power profile is forced to stay within the range of the chosen p_{max} by using Eq. (12).

$$p_{t,y}^g = P_{t,y}^{g,profile}\cdot p_{max}^g \quad (11)$$

$$p_{t,y}^g \leqslant p_{max}^g \quad (12)$$

2.2.6. BESS constraints

The BESS power capacity is calculated using a power-energy ratio parameter, with the BESS energy capacity representing the decision variable, as seen in Eq. (13). This BESS power capacity limits the charging and discharging capacities as seen in Eqs. (14) and (15).

$$p_{max}^s = \frac{e_{max}^s}{PE_{ratio}} \quad (13)$$

$$p_{t,y}^{sch} \leqslant p_{max}^s \quad (14)$$

$$p_{t,y}^{sdis} \leqslant p_{max}^s \quad (15)$$

The BESS energy balance is shown in Eq. (16), where charging and discharging efficiencies are included depending on the battery technology. Eq. (17) constrains the energy capacity of the BESS by minimum and maximum value. Also, energy losses related to the actual depth of discharge and discharging amount are included in the balance (penalizing the BESS efficiency when it has a low charge and has high charging or discharging values). These are calculated by Eqs. (18) and (19), in which the higher value from both is used. By setting these equations, the BESS is maintained healthier (operating at fuller state-of-charge and not having drastic energy charges or discharges).

$$e_{t,y}^s = e_{(t-1),y}^s + \eta^{sch}\cdot p_{t,y}^{sch}\cdot dt - \frac{p_{t,y}^{sdis}\cdot dt}{\eta^{sdis}} - e_{t,y}^{sloss} \quad (16)$$

$$e_{min}^s = Soc_{min}\cdot e_{max}^s \leqslant e_{t,y}^s \leqslant e_{max}^s \quad (17)$$

$$e_{t,y}^{sloss} \geqslant 0.2 p_{t,y}^{sdis}\cdot dt \quad (18)$$

$$e_{t,y}^{sloss} \geqslant \frac{0.2 e_{t,y}^s}{(Soc_{min} - 1)\cdot PE_{ratio}} + \frac{0.2 p_{max}^s\cdot dt}{1 - Soc_{min}} \quad (19)$$

2.2.7. Energy balance

Eq. (20) represents the energy balance of the system. This corresponds to the sum of every energy input and output which has to be equal to the SAG mill's energy consumption already transformed as a power input.

$$p_{t,y}^g - p_{t,y}^{sch} + p_{t,y}^{sdis} + p_{t,y}^{imp} - p_{t,y}^{exp} = P_{t,y}^{SAG} \quad (20)$$

Eqs. (21) and (22) establish the maximum imported power from the grid. It is defined as the maximum from every year y. If there is power over-consumption, $p_y^{max,imp}$ will be greater than the contracted power and penalties will apply. If there is no over-consumption, $p_y^{max,imp}$ will be equal to the contracted power so that penalties will not apply.

$$p_{t,y}^{imp} \leqslant p_y^{max,imp} \quad (21)$$

$$p^{con} \leqslant p_y^{max,imp} \quad (22)$$

2.2.8. Input data

The SAG mill power consumption data is generated using the mining model by generating different realizations of yearly mineral extraction data using geostatistics modeling (generating truck loads feeding the mineral processing plant). These truck loads have a specific energy consumption so they can be transformed to power values associated to the ore that feeds the SAG. The PV power generation data is obtained using the solar model by generating synthetic solar years from actual data. These values are a direct input to the optimization model at a 5 min time resolution, representing truck loads of ore fed to the mill for six months.

The model is designed to be general enough to support any kind of storage. For this case, Li-ion batteries are considered as the primary storage with a 20-year lifespan. The investment cost for the PV system and BESS are projected for the year 2020 (Child et al., 2017). The investment costs are considered as annuities, calculated with a 4% interest rate for 20 years.

Table 4 shows the values used for the simulations. These values are highly variable and are case specific.

2.3. Solar years variability impact study

Different solar years provide, on average, similar values in terms of the total yearly produced energy. The main differences occur in how the bad days are distributed within the years. For example, it makes a

Table 4
Optimization input parameters values.

Parameter	Value
C^{imp}	85 US$/MWh
C^{exp}	75 US$/MWh
C^{con}	120,000 US$/MW
$C^{penalty}$	180,000 US$/MW
PE_{ratio}	4 MWh per MW
N_{max}^{cycles}	3000 cycles
Soc_{min}	30%
$C^{rep,s}$	127.4 US$/MWh
η^{sch}	97%
η^{sdis}	95%
Inv^g	885 US$/MWp[a]
Inv^s	363.2 US$/MWh
$C^{op,g}$	1 US$/MW

[a] MWp refers to the maximum power output of a PV plant.

difference whether there are several cloudy days in a row or whether these are scattered over the year.

The impact of different solar years is studied by simulating one year at a time, arbitrarily choosing a year with several bad days in a row (cloudy year) and an average year regarding generation and without long cloudy day sequences. These simulations are made on a single arbitrary realization of the mineral feed taken from the geometallurgical model to solely study the investment impact. Because the PV plant and BESS investment are done only once, their sizing must be such that it works considering the variability in power requirements due to the different solar years. Therefore, it is also considered a simulation including several different solar years in a stochastic optimization, but still using the same mineral feed scenario.

Three cases are assessed:

1. Average year: This case uses an average year selected arbitrarily from the real records. This is chosen by comparing the overall power generation and selecting the one that has an average power generation (from the 13 years of data) and that has no cloudy day sequence. The selected record is the year 2006. This is used as a base case.
2. Cloudy year: This case uses a cloudy year selected arbitrarily from the actual records. This is chosen by selecting the year which has the largest amount and most extended contiguous cloudy day sequence (3 sequences of two bad days in a row, 1 sequence of three bad days in a row and 2 of four bad days in a row), although this is not the one that has the largest amount of cloudy days through the year. This year has an average power generation. The selected record is the year 2016.
3. Stochastic case: This case uses 20 synthetic years generated using the solar model to introduce variability in the simulation.

The simulations were run on a computer with a 3.6 GHz octa-core processor and 16 GB of RAM. Each simulation instance takes in average 3 h to run.

3. Results and discussion

3.1. Model testing

The model provides operational and investment decisions. A typical operation day profile is depicted in Fig. 4. This shows how the model works and how the PV-BESS system interacts with the power imports. As expected, it is found that during daylight time, the PV-BESS system matches the mill's load, and the battery is charged; at night, the stored energy is used together with the power imports from the grid to cover demand. The power contract is used very steadily, without exceeding the contract limit.

In general terms, the optimal plant size allows the SAG mill to be energy-autonomous during the months with abundant irradiance, while the power grid supports the operation mainly during winter for all solar scenarios. This behavior can be seen in Fig. 5, in which the solar power generation decreases and the imported grid power rises on winter. The BESS behavior is also affected in winter, where it charges more slowly. Also, the system is less dependent on it. The grid and BESS power graph show how they are a perfect complement during the day and night. Cloudy days can also be seen in the PV power graphs as white stripes. In those days, the grid provides the energy.

3.2. Investment decisions

Frequently, system planning is done using average meteorological years. However, not every "average" year is the same. A year with a long sequence of cloudy days generates dramatic impacts on the operation and all investment recommendations, but more strongly on the BESS as shown in Fig. 6 (gray bars). This behavior is contrary to what happens when sizing autonomous PV systems using the worst-week criteria (i.e., choosing the worst week from the typical meteorological year). Here, the BESS energy capacity is almost halved, in a trade-off with a larger power contract and energy imports.

Using stochastic optimization, the solar uncertainty and its variability (and involved risk) is accounted for. Modeling the system considering several years yields a different result than the average year (blue bars on Fig. 6). The obtained PV-BESS system is smaller, where a notorious difference occurs in the BESS investment decision. Because of the latter, the needed contracted power is higher, implying higher net imports to make full use of it. The power contract acts as a trade-off with the PV-BESS investment decision, as the system needs to take more energy from the grid to cover the lower solar energy available.

When comparing the results obtained, the stochastic case acts as an intermediate solution. It is more conservative than the average case, but not as extreme as the cloudy day sequence scenario. This is because it

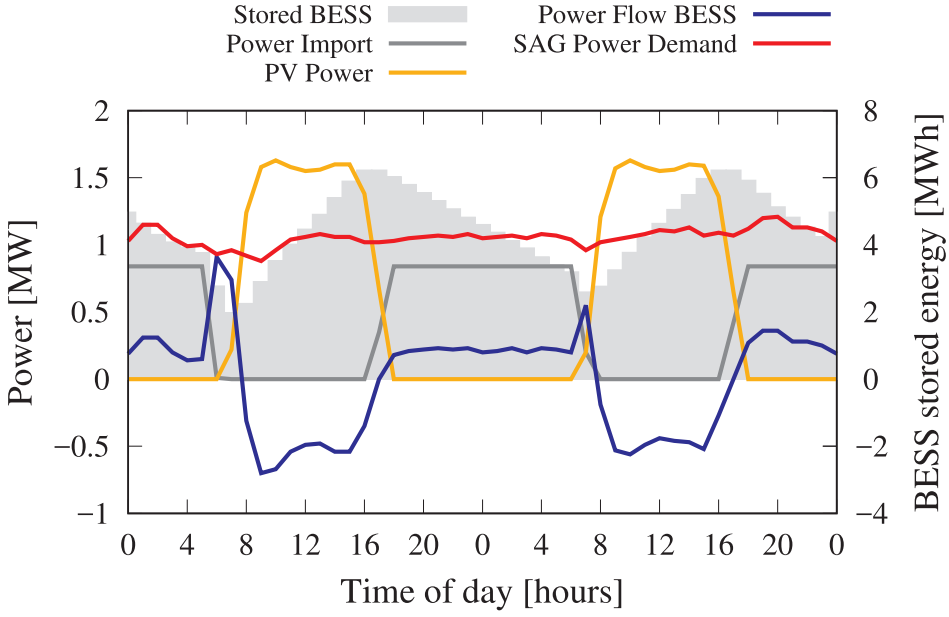

Fig. 4. Operation behavior of the SAG-PV-BESS system.

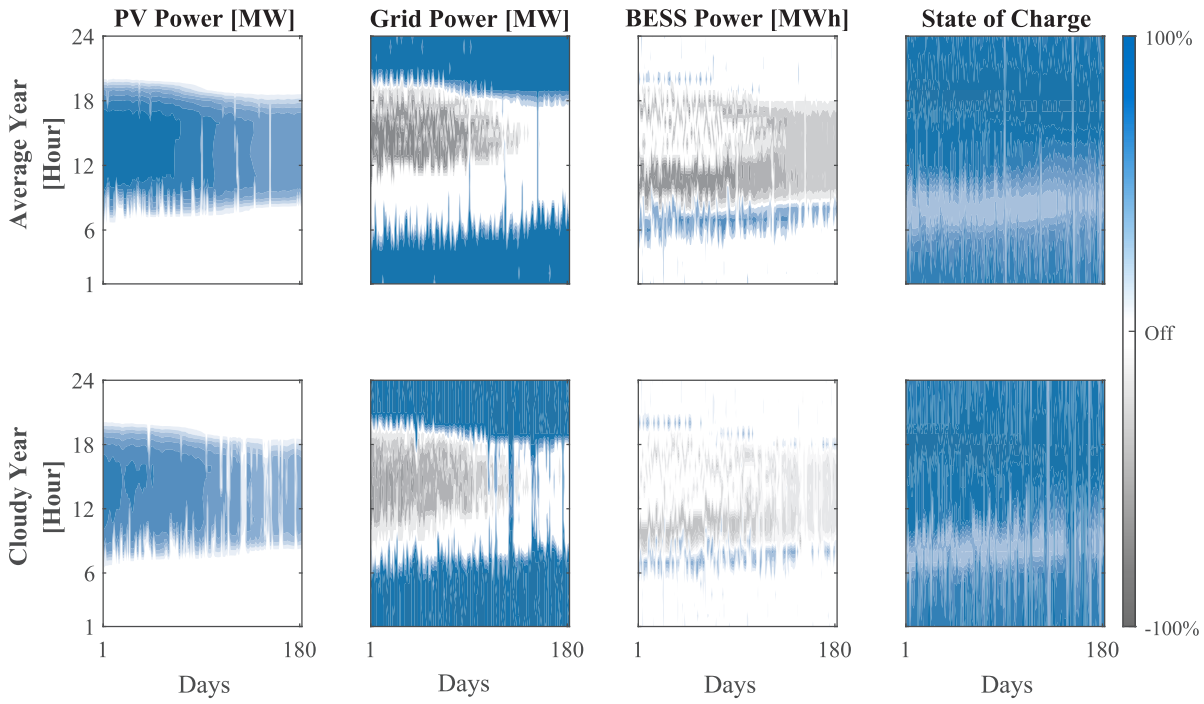

Fig. 5. Six month of operation of the power grid and the PV-BESS system for an average and cloudy year. Gray represents net flow of energy to the grid or BESS, while blue represents net flow of energy from the PV, BESS or grid. (For interpretation of the references to color in this figure legend, the reader is referred to the web version of this article.)

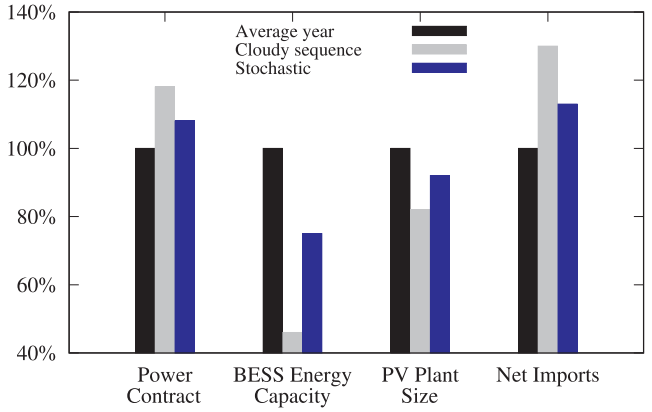

Fig. 6. Impact of using an average solar year, a cloudy solar year (prolonged cloudy sequence) and many solar years on the optimal sizes. Values relative to the average year.

finds a solution that fits the best investment decision to balance between years with long cloudy day sequences and good solar years.

For the results, it is found that penalties are unlikely to occur since the optimization is choosing a power contract that avoids having this extra cost, since it is cheaper to have a higher contracted power than paying the penalties.

3.3. Mineral variability

Solar irradiation has an impact on the design, but other parameters may affect the system sizing. In the previous simulations, the mineral feed (using its mineral hardness variability as an input) remained constant, so it is of interest to compare the previous results with those obtained with a different feed. This feed can have either a lower or higher variability of rock hardness and, hence, of specific energy consumption. Generating synthetic feeds allows several scenarios to be studied and assessed within the simulation to obtain robust results. Using Eq. (23), the variance of the original feed's hardness is amplified or diminished while maintaining its average value.

$$y_2 = (y_1 - \overline{y_1})\cdot\alpha + \overline{y_1} \quad (23)$$

where

- y_2 is the modified value (resulting amplified or diminished feed's SEC values)
- y_1 is the base value (original feed's SEC values)
- $\overline{y_1}$ is the average value of the base case
- α is the standard deviation modification factor

The results for the new simulations are shown in Table 5. These show a clear trend with feed variability. Especially the BESS energy capacity is highly affected by the feed variability. With a higher variability, the needed BESS rises, and the opposite occurs with lower feed variability. As consequence, understanding in more detail the variability of the ore-feed and how to control it, seems to be a relevant research questions for the future. In light of the large energy storage backup that the power systems will need (for accommodating large shares of renewable generation), it is imperative to understand how the mine can contribute with flexibility. This leads to further questions about the effects of other characteristics of the mineral feed's hardness such as its uncertainty, form and magnitude of the variability that it has when fed to the mill.

The context in which the PV-BESS integration is planned has a direct

Table 5
Impact of a increasing or decreasing the ore variability on the optimal sizes.

	Base Case (α = 1)	α = 1.5	α = 1.25	α = 0.75	α = 0.5
Power Contract	100%	102%	101%	99%	98%
BESS Energy Capacity	100%	150%	120%	80%	50%
PV Plant Size	100%	103%	101%	99%	97%
Grid Imports	100%	98%	99%	101%	102%
Total Costs	100%	101%	100%	100%	99%

Table 6
Solar days classification ranges.

Class	Range	Jan	Feb	Mar	Apr	May	Jun
Excelent	100–95%	26 (6%)	91 (25%)	54 (13%)	46 (12%)	50 (12%)	26 (7%)
Good	95–85%	255 (63%)	239 (57%)	169 (59%)	208 (43%)	297 (52%)	210 (76%)
Moderate	85–60%	118 (29%)	61 (17%)	106 (26%)	159 (41%)	111 (28%)	38 (10%)
Bad	60–0%	4 (1%)	6 (2%)	4 (1%)	16 (4%)	34 (8%)	29 (7%)
Max. Daily Irradiation	kWh	10.2	9.4	8.8	7.6	6.3	5.5
Class	Range	Jul	Aug	Sep	Oct	Nov	Dec
Excelent	100–95%	18 (4%)	69 (17%)	46 (12%)	46 (11%)	110 (28%)	51 (13%)
Good	95–85%	263 (65%)	171 (42%)	226 (58%)	240 (60%)	200 (51%)	228 (57%)
Moderate	85–60%	98 (24%)	147 (36%)	115 (29%)	111 (28%)	80 (21%)	117 (29%)
Bad	60–0%	24 (6%)	16 (4%)	3 (1%)	6 (1%)	0 (0%)	3 (1%)
Max. Daily Irradiation	kWh	6.0	7.1	8.5	9.6	10.0	10.4

relation to how effective it will be. In this case, only the SAG mill consumption is being considered with its variability. It could be that, when considering the complete mineral variability, the solution changes. For further refinement, the SAG mill's power demand could be modelled dynamically. However, the results presented here show a trend that is not expected to change by using a better model, but only be more precise.

4. Conclusions

A novel framework was developed for optimal sizing of a solar photovoltaic and a battery energy storage system to supply energy for a SAG mill (SAG-PV-BESS), in copper mining, with grid backup. This framework consists of a mining model (mineral extraction sequencing by using geostatistics) and a solar model (generation of time series of solar radiation) which generate data to feed the optimization model that sizes the PV-BESS system according to the power needs.

The proposed model allows determining the best sizes of the PV, BESS, and power contract. It considers a whole year (static planning) with hourly resolution, and uses multiple yearly solar times series as inputs. These time series are generated with the solar model, which is based on Markov Chains. After developing these models, the impact of different solar years on the system sizes is studied. Additionally, the effect of amplifying the variability of the mineral feed on the optimal sizes is assessed. The model results obtained are highly plausible, and in the base case it can be seen how PV-BESS provides a cost-effective solution for energy provision.

Using different solar years has a significant impact on the sizing and total costs for each scenario. Three cases are compared, using: an average year (average solar energy, average cloudy day sequence), a year with long cloudy day sequence (but still with average solar energy), and a stochastic optimization using many solar years in one simulation. Long cloudy sequences have a significant impact on the sizing of the PV-BESS system, and the SAG mill relies more strongly on imports (lower solar autonomy). The stochastic optimization resulted in an intermediate solar autonomy. A higher variability in the mineral hardness also strongly impacts the optimal sizes. Also, the knowledge of the solar resource shows to be crucial for correct sizing of the PV-BESS system. Stochastic planning inherently makes the results more robust.

There is a strong relationship between the variability of the mineral hardness and the required PV-BESS system sizing. Therefore, it is important to have a correct estimation of the mineral that is extracted (and fed to the processing plant) and how variable this will be in this stage. By taking this idea one step further, one could control the feed, and achieve even larger cost reductions in the energy supply. This motivates a second study (Pamparana et al., 2019) in which the mineral variability and uncertainty are going to be studied regarding on how this impacts the optimal system size.

Acknowledgments

This work was supported by the Chilean National Commission for Scientific and Technological Research (CONICYT), through the SERC-Chile (CONICYT/FONDAP/15110019) and the Solar Mining project (CONICYT-BMBF 20140019), the German Academic Exchange Service (DAAD), and the German Research Foundation (DFG-NO 805/11-1). The authors also acknowledge the support of the Natural Sciences and Engineering Research Council of Canada (NSERC), funding reference number RGPIN-2017-04200 and RGPAS-2017-507956.

Appendix A. Historical solar days classification

Table 6 shows the actual classification obtained from the historical data including the number of days for each month in each class. Also, the maximum daily irradiation for each month is shown.

References

Alruiz, O., Morrell, S., Suazo, C., Naranjo, A., 2009. A novel approach to the geometallurgical modelling of the Collahuasi grinding circuit. Miner. Eng. 22 (12), 1060–1067.

Amelunxen, P., Mular, M., Vanderbeek, J., Hill, L., Herrera, E., 2012. The effects of ore variability on HPGR trade-off economics. In: Proceedings of International Autogenous

and Semiautogenous Grinding Technology 2011. Canadian Institute of Mining, Metallurgy and Petroleum.
Bergholz, W.S., Schreder, M., 2003. Escondida—Phase IV grinding circuit. In: 36th. Annual Meeting. The Canadian Institute of Mining, Metallurgy and Petroleum.
Bueno, M., Foggiatto, B., Lane, G., 2015. Geometallurgy applied in comminution to minimize design risks. In: Proceedings SAG Conference, Vancouver, Canada, May 2015.
Burger, B., McCaffery, K., Jankovic, A., Valery, W., McGaffin, I., 2006. Batu Hijau model for throughput forecast, mining and milling optimisation and expansion studies. Adv. Comminution 3, 461–479.
Carrasco, C., Keeney, L., Napier-Munn, T., 2016. Methodology to develop a coarse liberation model based on preferential grade by size responses. Miner. Eng. 86, 149–155.
Castillo, P., Kouro, S., Rojas, C.A., Muller, N., 2015. Photovoltaic DC-DC converter for direct power interface to copper electrorefining process. In: Industrial Electronics Society, IECON 2015-41st Annual Conference of the IEEE. IEEE, pp. 004388–004393.
Cebulla, F., Haas, J., Eichman, J., Nowak, W., Mancarella, P., 2018. How much electrical energy storage do we need? A synthesis for the US, Europe, and Germany. J. Clean. Prod. 181, 449–459.
Child, M., Breyer, C., Bogdanov, D., Fell, H.-J., 2017. The role of storage technologies for the transition to a 100% renewable energy system in Ukraine. Energy Procedia 135, 410–423.
COCHILCO, 2013. Actualización de información sobre el consumo de energía asociado a la minería del cobre al año 2012. Tech. rep. COCHILCO < www.cochilco.cl > .
Cruz-Robles, I., Vaamonde, A.J.V., Alonso, E., Pérez-Rábago, C.A., Estrada, C.A., 2018. Potential of solar central tower systems for thermal applications in the production chain of copper by pyrometallurgical route. In: AIP Conference Proceedings, vol. 2033. AIP Publishing, pp. 020002.
Flores, L., 2005. Hardness model and reconciliation of throughput models to plant results at Minera Escondida LTDA, Chile. In: 37th Annual Meeting of the Canadian Mineral Processors, Ottawa.
Gulagi, A., Bogdanov, D., Fasihi, M., Breyer, C., 2017. Can Australia power the energy-hungry Asia with renewable energy? Sustainability 9 (2), 233.
Haas, J., Cebulla, F., Cao, K., Nowak, W., Palma-Behnke, R., Rahmann, C., Mancarella, P., 2017. Challenges and trends of energy storage expansion planning for flexibility provision in low-carbon power systems–a review. Renew. Sustain. Energy Rev. 80, 603–619.
Haas, J., Olivares, M., Palma-Behnke, R., 2015. Grid-wide subdaily hydrologic alteration under massive wind power penetration in Chile. J. Environ. Manage. 154, 183–189.
Han, X., Ji, T., Zhao, Z., Zhang, H., 2015. Economic evaluation of batteries planning in energy storage power stations for load shifting. Renew. Energy 78, 643–647.
Harmsen, J., Roes, A., Patel, M.K., 2013. The impact of copper scarcity on the efficiency of 2050 global renewable energy scenarios. Energy 50, 62–73.
Jahani, M., Noaparast, M., Farzanegan, A., Langarizadeh, G., 2012. Application of SPI for Modeling energy consumption in Sarcheshmeh SAG and ball mills. J. Min. Environ. 2 (1).
Keeney, L., Walters, S., Kojovic, T., 2011. Geometallurgical mapping and modelling of comminution performance at the Cadia East porphyry deposit. In: GeoMet 2011-1st AusIMM International Geometallurgy Conference 2011. AusIMM: Australasian Institute of Mining and Metallurgy, pp. 73–83.
Kittler, P., Liebezeit, V., Ehrig, K., Macmillan, E., Lower, C., 2011. It seemed like a good idea at the time… Common mistakes in geometallurgy. In: Proceedings of First International AusIMM Geometallurgical Conference, Brisbane, Australia.
Kojovic, T., Michaux, S.P., Walters, S., 2010. Development of new comminution testing methodologies for geometallurgical mapping of ore hardness and throughput. In: XXV International Mineral Processing Congress 2010, IMPC 2010 2, pp. 891–899.
Kondziella, H., Bruckner, T., 2016. Flexibility requirements of renewable energy based electricity systems–a review of research results and methodologies. Renew. Sustain. Energy Rev. 53, 10–22.
Koskinen, O., Breyer, C., 2016. Energy storage in global and transcontinental energy scenarios: a critical review. Energy Procedia 99, 53–63.
McLellan, B., Corder, G., Giurco, D., Ishihara, K., 2012. Renewable energy in the minerals industry: a review of global potential. J. Cleaner Prod. 32, 32–44.
Ministerio de Energía de Chile, 2017. Explorador solar. Available online: < http://walker.dgf.uchile.cl/Explorador > (accessed on 22 September 2018).
Molina, A., Falvey, M., Rondanelli, R., 2017. A solar radiation database for Chile. Sci. Rep. 7 (14823), 1–11.
Norgate, T., Haque, N., 2010. Energy and greenhouse gas impacts of mining and mineral processing operations. J. Cleaner Prod. 18 (3), 266–274.
Norgate, T., Jahanshahi, S., 2010. Low grade ores–smelt, leach or concentrate? Miner. Eng. 23 (2), 65–73.
Pamparana, G., Kracht, W., Haas, J., Díaz-Ferrán, G., Palma-Behnke, R., Román, R., 2017. Integrating photovoltaic solar energy and a battery energy storage system to operate a semi-autogenous grinding mill. J. Cleaner Prod. 165, 273–280.
Pamparana, G., Kracht, W., Haas, J., Ortiz, J., Nowak, W., Palma-Behnke, R., 2019. Studying the integration of solar energy into the operation of a semi-autogenous grinding mill. Part II: Effect of ore hardness variability and geometallurgical modeling and management. Miner. Eng.
Rahmann, C., Vittal, V., Ascui, J., Haas, J., 2016. Mitigation control against partial shading effects in large-scale PV power plants. IEEE Trans. Sustain. Energy 7 (1), 173–180.
Ren21, et al., 2018. Global Status Report. REN21 Secretariat, Paris.
Schill, W.-P., Zerrahn, A., 2018. Long-run power storage requirements for high shares of renewables: results and sensitivities. Renew. Sustain. Energy Rev. 83, 156–171.
Starkey, J., Dobby, G., 1996. Application of the Minnovex SAG power index at five Canadian SAG plants. In: Proceeding Autogenous and Semi-Autogenous Grinding, pp. 345–360.
Starkey, J., Scinto, P., 2010. SAG Mill grinding design versus geometallurgy–getting it right for competent ores. In: Proceedings of 25th Inter-national Mineral Processing Congress. Brisbane: AusIMM, pp. 1265–1271.
Steinke, F., Wolfrum, P., Hoffmann, C., 2013. Grid vs. storage in a 100% renewable Europe. Renew. Energy 50, 826–832.
Suazo, C., Kracht, W., Alruiz, O., 2010. Geometallurgical modelling of the Collahuasi flotation circuit. Miner. Eng. 23 (2), 137–142.
Topp, V., 2008. Productivity in the mining industry: measurement and interpretation. Tech. Rep. Productivity Commission Staff Working Paper. Government of the Commonwealth of Australia – Productivity Commission. <www.pc.gov.au/research/supporting/mining-productivity>.
Toscano, R., 2013. Structured Controllers for Uncertain Systems: A Stochastic Optimization Approach. Springer Science & Business Media, London.
US Department of Energy, 2018. DOE Global Energy Storage Database.
Viveka, R., Kalyani, S., Devie, P., 2015. Optimal planning of energy storage systems in transmission networks using evolutionary algorithm. Int. J. 83, 87–97.
Wei, D., Craig, I.K., 2009. Grinding mill circuits—a survey of control and economic concerns. Int. J. Miner. Process. 90 (1), 56–66.
Wirfiyata, F., McCaffery, K., 2011. Applied geo-metallurgical characterisation for life of mine throughput prediction at Batu Hijau. In: Fifth International Conference on Autogenous and Semiautogenous Grinding Technology, Canadian Institute of Mining, Metallurgy and Petroleum, Vancouver, Canada.
Zerrahn, A., Schill, W.-P., 2017. Long-run power storage requirements for high shares of renewables: review and a new model. Renew. Sustain. Energy Rev. 79, 1518–1534.